CARLO MANGANO[1], JAMIL AWAD SHIBLI[2], FRANCESCO MANGANO[3], RACHEL SAMMONS[4], ALDO MACCHI[1]

[1]University of Varese, Italy
[2]University of Guarulhos, Sao Paulo, Brasil
[3]Private Practice, Gravedona (Como), Italy
[4]University of Birmingham, UK

Dental implants from laser fusion of titanium microparticles: from research to clinical applications

ABSTRACT

Dental implants currently available on the market are conventionally produced by machining titanium rods, with subsequent application of surface treatments or coatings, with the aim to accelerate the bone healing process. The progress in the field of rapid prototyping technology makes it possible to modulate the elastic properties of the implants to those of surrounding bone. The direct laser fabrication (DLF) allows solids with complex geometry to be produced by focusing metal powder microparticles in a laser beam, according with a computer three-dimensional (3D) model. For dental implants, the fabrication process involves the fusion, through a computer guided laser beam, of titanium microparticles, in order to realise, layer by layer (each one with a thickness of 20 Ìm) the desired object. Our Research Group, first in the world, has developed a method to produce dental implants using a laser fusion of titanium microparticles. With this method it is possible to create, regulating the settings of the different layers, implants with graduated and controlled porosity, incorporating a gradient of porosity, from the inner core to the outer surface. On the one hand, this kind of modulation can allow a better load adaptation and distribution; on the other hand, the new porous surface can promote the bone healing process. The new implants obtained from the fusion of titanium microparticles show a surface with a repetitive sequence of concavities, which are directly connected to the underlying porous spaces. This kind of geometry, rich in interconnected pores, has demonstrated in previous works to induce a good biological response in vitro. The aim of the present study was to test the biological behaviour of the new implants obtained from the fusion of titanium microparticles (TixOs, Leader-Novaxa, Milan, Italy) in vivo, in human type IV bone, after an unloaded healing period of two months.

Keywords Dental implants, direct laser fabrication, implants obtained from the fusion of titanium microparticles, controlled porosity, concavities.

INTRODUCTION

Dental implants currently available on the market are manufactured from commercially pure titanium or titanium alloy Ti-6Al-4V (90% titanium, 6% aluminum, 4% vanadium). They are produced by machining titanium rods, with subsequent application of surfaces treatments or coatings, with the aim to accelerate the bone healing process (1). Although the titanium alloy has demonstrated superior physical and mechanical properties, commercially pure titanium has always been considered the material of choice in implant dentistry, because of its excellent ductility, corrosion resistance and biocompatibility (1-2). The elastic properties of conventional dental implants, however, are different from those of surrounding bone (1,3-6). The stiffness of a dental implant depends intrinsically on the elastic module (Young's modulus) of the employed material, as well as by the geometric properties of the implant itself. The elastic modulus of commercially pure titanium (112 GPa) and of titanium alloy Ti-6Al-4V (115 GPa) are considerably higher than that of cortical bone (10-26 GPa). This big difference can lead to stress shielding of the residual

bone, which can lead to the risk of detrimental resorptive bone remodelling (1,3-7). This problem is often disregarded but it is of paramount importance in modern oral implantology, where clinical needs are more often oriented to early or immediate loading protocols (4-7). In the last years, however, the extraordinary advances in the field rapid prototyping (RP) enabled us to modulate the elastic properties of the Ti-6Al-4V implants to those of surrounding bone. The direct laser forming (DLF) allows solids with complex geometry to be produced by focusing metal powder microparticles in a laser beam, according with a computer three-dimensional (3D) model (8-11). For dental implants, the fabrication process involves the fusion, through a computer guided laser beam, of titanium microparticles, in order to realise, layer by layer (each one with a thickness of 20 Ìm) the desired object. Our Research Group, first in the world, has invented a method to produce dental implants using a laser fusion of titanium microparticles (1,9,11). With our method it is possible to create, regulating the settings of the different layers, implants with graduated and controlled porosity, incorporating a gradient of porosity, from the inner core to the outer surface. On the one hand, this kind of modulation can guarantee a better load distribution, allowing a gradual mechanical adaptation of the implant to surrounding bone (7-10); on the other hand, the new porous surface can promote the bone healing process, enhancing the mechanical interconnection between the bone and the implant (8-11). The integration of the implant into the bone is a fundamental biological step, and the quest for new implant surface geometries is one of the most important topics in the modern oral implantology. At the beginning, researchers focused their attention on the concept of surface roughness (12-16), because a rough surface can promote a larger and faster bone apposition, when compared to a machined one (12-16). From a study of 12 different implant surfaces evaluating the different implant properties which could potentially influence bone apposition, Thomas and Cook (12) concluded that only the microtopographical aspect was really able to affect osseointegration. Wong (13) e Carlsson (14) reported that a surface with a roughness (Ra) comprised between 1 and 10 Ìm is optimal in promoting new bone apposition, stimulating the commitment of mesenchymal stem cells into functional osteoblasts. Wennenberg (15) e Boyan (16) demonstrated that the production of bone matrix and soluble signals (TGFbeta-1, PGE-2, and many others) was strictly correlated to the surface roughness. Hydroxylation, hydratation, absorption of cations and anions (calcium and phosphate) and biomolecules (proteins, glycoproteins, glycolipids, proteoglycans e polysaccharides), with a temporary formation of a well established fibrin clot, are the first event occurring at the bone-implant interface (17-18). All these events are mediated by the formation onto the implant surface of a stable oxide layer, which is capable to guarantee, through its peculiar properties (lower ions concentration, dielectric constant similar to that of water and slightly negative charge at physiological pH levels) an ideal interaction with the biological fluids (17-20). Rough surfaces have demonstrated better biomolecule adsorption from biological fluids, due to their superior surface area, free energy and wettability (19-20). Cell adhesion is mediated by an amorphous, not homogeneous layer (from 50 to 600 nanometers thick) composed by proteoglycans, glycoproteins, bone sialoproteins (BSP) and osteopontin (OPN). In particular, bone sialoproteins can favour the differentiation of mesenchymal stem cells into functional osteoblasts, while osteopontin mediates focal cell adhesion

(22) through a specific RGD sequence (23). As we will see, the mechanism of focal cell adhesion triggers a series of events modulating the new bone formation on the implant surface (23-24). As previously demonstrated (1,9,11), direct laser metal forming (DLMF) implants initially show a great number of roughly spherical particles and microspheres weakly adherent to their surface. These spheres are remnants of the original powders (8-11). After a specific treatment using an organic acid mixture (Leader-Novaxa, Milan, Italy), however, the surface of the implants appear completely different, revealing an homogenous surface geometry, rich in concavities. These cavities, of variable diameter (100-200 Ìm) extend beneath the surface, communicating with the porous spaces of which the outer implant portion is rich; these pores are and interconnected through channels and tunnels. This peculiar geometry can be obtained only through the laser microfusion procedure (1,9,11). In fact, this surface is no longer a rough, but instead a porous one, and this fact has been demonstrated through morphological characterization with scanning electron microscopy supported by three dimensional reconstruction with applied softwares (11). Our Research Group has initially tested the biological response to this specific surface in vitro, investigating the human fibrin clot formation as well as the osteoblast behaviour (1,9,11). After a 5 minutes contact with human blood, the scanning electron microscopy investigation revealed the ability of this surface to induce the formation and organization of a diffuse, three dimensional fibrin network (11). Osteoblast cells study revealed major cell density inside the concavities. On the one hand, cells spanned across intervening crevices, by means of extended tightly stretched processes; on the other hand, cells penetrated into the bigger cavities, in which initial deposition of bone matrix was shown (11). The aim of the present study was to test the biological behaviour of the new DMLF surface implants (TixOs, Leader-Novaxa, Milan, Italy) in vivo, in human type IV bone, after an unloaded healing period of two months. It was our intention to evaluate the quantity and quality of bone apposition on the new surface of DLMF implants, through an histologic and histomorphometric study. The surface of the DLMF implants was compared with two different surfaces of conventional implants actually on the market (Conexao Implants, Sao Paulo, Brasil), as a machined surface (cpTi) and a sandblasted, acid etched surface (SAE), used as controls. In addition, the DLMF surface was evaluated with scanning electron microscopy and x-ray dispersive spectrometry.

MATERIALS AND METHODS

Patients selection

Thirty patients (20 women; 10 men), with a mean age of 51.3 ±3.0 years, referred to the Department of Periodontology, Dental Research Division, Guarulhos University, Sao Paulo, Brazil, for oral rehabilitation with dental implants, were enrolled in this study. The patients were totally edentulous, with a need of complete rehabilitation with full arch prosthesis supported by implants. Exclusion criteria included pregnancy, nursing, heavy smoking habits (more than 15 cigarettes/day), and any systemic condition that could affect bone healing. All patients were properly informed about the study, signing a specific consent form. The Ethics Committee for Human Clinical Trials at Guarulhos University approved the study protocol (CEP-UnG# 201).

Preparation of test implants

Ten screw-shaped mini-implants were

manufactured from titanium alloy (Ti-6Al-4V) with DLMF technique (Leader-Novaxa, Milan, Italy). The DLMF implants were made of master alloy powder, with a particle size of 25-45 µm as the basic material. The implants were 2.0 mm in diameter and 8.0 mm in length. Processing was carried out in an argon atmosphere using a powerful Yb (Ytterbium) fiber laser system (EOS GmbH Munchen, Germany) with the capacity to build a volume up to 250 mm ? 250 mm ? 215 mm using a wavelength of 1054 nm with a continuous power of 200 W, at a scanning rate of 7 m/s. The size of the laser spot was 0.1 mm. To remove residual particles from the manufacturing process, the samples were sonicated for 5 min in distilled water at 25°C, immersed in NaOH (20 g/L) and hydrogen peroxide (20 g/L) at 80° C for 30 min, and then further sonicated for 5 min in distilled water. Acid etching was carried out by immersion of the samples in a mixture of 50% oxalic acid and 50% maleic acid (Leader-Novaxa, Milan, Italy) at 80°C for 45 min, washing for 5 min in distilled water in a sonic bath.

Preparation of control implants

Twenty screw-shaped mini-implants (Conexao Implants, Sao Paulo, Brasil), obtained from conventional turning of titanium bars, were used as controls. Each mini-implant was 2.5 mm in diameter and 6.0 mm long. Implants were made of grade-4 titanium. Ten of these implants had a standard, machined surface (cpTi), with no surface modifications; the other were sandblasted, acid etched implants (SAE). After sandblasting with 25-100 µm TiO2 particles, the mini-implants were ultrasonically cleaned with an alkaline solution, washed in distilled water and pickled with a mixture of HNO3 and HF (Conexao Implants, Sao Paulo, Brazil) The acid etching process was controlled to create a homogeneous implant surface topography.

Mini implants surgery

Thirty screw-shaped mini-implants (n=10 DLMF, n=10 cpTi, n=10 SAE) were used in this study. Each patient received only 1 mini-implant, which was inserted in the posterior region of the maxilla, always distal to the last conventional placed implant. The micro-implants were placed under aseptic conditions. After crestal incision, mucoperiosteal flaps were raised and conventional implants were placed in the totally edentulous maxilla in accordance with the surgical/prosthetic plan prepared for each patient. Next, the mini-implant was placed in the molar region in a randomized way, posterior to the most distal conventional implant. The mini-implant recipient site was prepared with a 1.8 mm diameter twist drill in soft bone (type IV bone). All drilling and mini-implant placement procedures were completed under profuse irrigation with sterile saline. If the mini-implant showed low primary stability, a backup surgical site was prepared. The flaps were sutured to cover the micro-implants. Amoxicillin was administered (Augmentin, Glaxo-Smithkline Beecham, Brentford, UK) two times a day (2000mg/day) for a week, in order to avoid post-surgical infection. Pain was controlled administering nimesulide, 100 mg/day for two days (Aulin, Roche Pharmaceutical, Basilea, Switzerland). To enable subjects to control postoperative dental biofilm, 0.12% chlorhexidine rinses were prescribed (Chlorexidine, OralB, Boston, MA, USA), twice a day for 14 day.

Healing period and implant retrieval

The sutures were removed after 10 days. After a submerged healing period of 2 months, during the 2-stage surgery of the conventional implants, the mini-implants and the surrounding tissues were retrieved

with a 4.0-millimeter-wide trephine bur (Trephine Bur, Hu-Friedy International, Chicago, IL, USA), and the specimens were fixed by immediate immersion in neutral formalin at 4%.

Specimen processing and histological and histomorphometrical analyses

The biopsies were processed (Precise 1 Automated System®, Assing, Rome, Italy) to obtain thin ground sections, they were dehydrated in an ascending series of alcohol rinses and embedded in glycol methacrylate resin (Technovit® 7200 VLC, Kulzer, Wehrheim, Germany). After polymerization, the specimens were sectioned lengthwise along the larger axis of the implant, using a high-precision diamond disk, to about 150µm, and ground down to about 30µm (Precise 1 Automated System, Assing, Rome, Italy). One to two slides were obtained from each implant. The slides were stained with basic fuchsin and toluidine blue. The histological analysis was performed using a light microscope (Laborlux S®, Leitz, Wetzlar, Germany) connected to connected to a high-resolution video camera (3CCD®, JVC KY-F55B, Milan, Italy) and interfaced to a monitor and personal computer AMD 1800 Mz. This optical system was associated with a digitizing pad (Matrix Vision GmbH, Milan, Italy) and a histometric software package with image-capture functionalities (Image-Pro Plus® 4.5, Media Cybernetics Inc., Immagini & Computer Snc, Milan, Italy). This system allowed to exactly quantify the percentages of titanium, bone tissue and bone marrow spaces in the examined specimens. In particular, three different histomorphometrical variables were taken into account:

- BIC% ("bone to implant contact"), defined as the amount of mineralized bone in direct contact with the implant surface, throughout the entire extent of the mini-implant.
- BDTA% ("bone density in the threaded area"), defined as the fraction of mineralized bone tissue within the threaded area. All threads were measured.
- BD% ("bone density"), defined as the bone density in a 300 µm-wide zone lateral to the implant surface.

The mean and standard deviation of histometric variables were calculated for each implant, then for each group of implants. Kruskall-Wallis and Dunn test were used to compare the surface topography as well as the histometric variables. The significance test was conducted at a 5% level of significance.

Scanning electron microscopy (SEM) and X-ray dispersive spectrometry

Two DLMF implant specimens were excised and fixed. The specimens were washed with Na-cacodylate buffer (pH 7.4), dehydrated in ascending ethanol and hexamethyldisilazane (Sigma-Aldrich Inc., Saint-Louis, MO, USA), sputter-coated with pure gold in an Emitech K550 apparatus (Quorum Technologies, Hailsham, UK) and mounted on appropriate stubs with carbon-based conductive adhesive. All specimens were observed under a FEI Philips XL30 FEG ESEM scanning electron microscopy (Philips, Amsterdam, The Netherlands) with secondary electrons and backscattered electrons operated at 7-15 kV. Pictures were directly acquired in digital format as 1424x968-pixel grayscale TIFF images. X-ray spectrometry was carried out on the same SEM fitted with an EDAX Sirion 200/400 apparatus and operated at 15 kV. Digital maps of the distribution of distinct elements were obtained in digital format as 512x512 BMP pictures. Selected maps were combined with the corresponding SEM micrographs in Adobe Photoshop (Adobe, San Jose, CA, USA).

RISULTATI

Clinical Observations

Four mini-implants (n=2 cpTi, n=1 SAE, n=1 DLMF) showed no osseointegration and were not included in the evaluation. These implants were excluded by the study. Twenty-six mini-implants were clinically stable at the time of retrieval. Neither of the remaining mini-implants presented marginal bone resorption or infection of the surrounding soft tissues. All these implants were used for this study. These implants were histologically and histomorphometrically evaluated. Two DLMF implants, moreover, were evaluated with scanning electron microscopy and x-ray spectrometry.

Histologic and histometric results

Overall, the bone surrounding the three surface topographies (cpTi, SAE e DMLF) was healthy. All the specimens showed the presence of remodeling activity in the bone next to the mini-implants. Woven bone with several osteocyte lacunae and preexisting bone were present; the woven newly formed bone was separated from the preexisting bone by cement lines. Osteoblasts were connected to the newly formed bone, showing ongoing bone formation. Substantial differences, however, were evidenced between the different surfaces. On the SAE (Fig. 1a-b) e DMLF (Fig. 2a-b) implants, the new bone was in direct contact with surface, showing early stages of maturing and remodeling; newly formed bone trabeculae were interposed between the preexisting bone and the implants (Fig. 2c). On the cpTi micro-implants, on the contrary, minor new bone apposition was observed, and the bone tissue appeared immature; some samples showed no connecting bridges between the new bone trabeculae and the implant surface. In these cases, bone trabeculae were separated from the machined surface by a thin layer of connective tissue (Fig. 3a-b). Histometric data confirmed these observations (Table

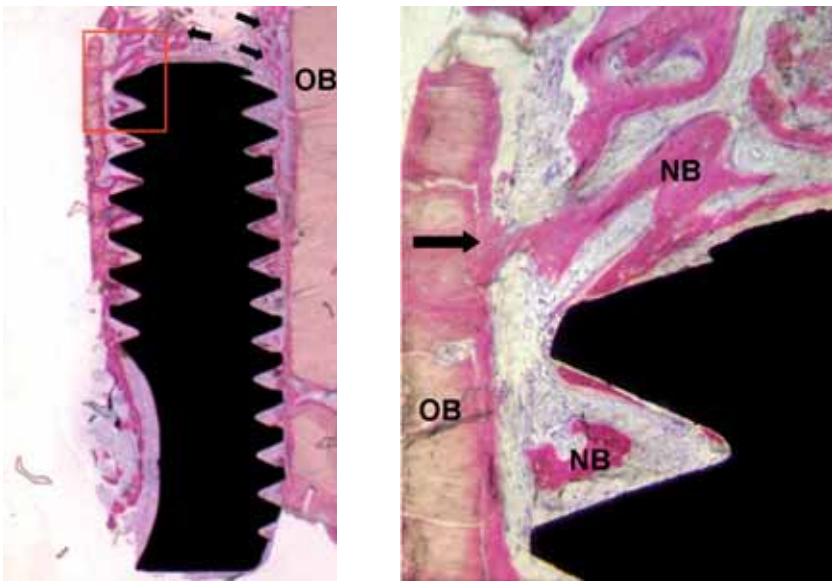

Fig. 1 SAE surface.

a Overview. New formed bone in adaned maturation and remodeling. The bone is in close contact with the implant surface (basic fuchsinr and toluidine blue 12 X).

a Higher magnification of the selected part of the preceding picture. The arrows indicate osteoblasts depositing bone, in some areas also in contact with the implant surface (basic fuchsin and toluidine blue 200 X).

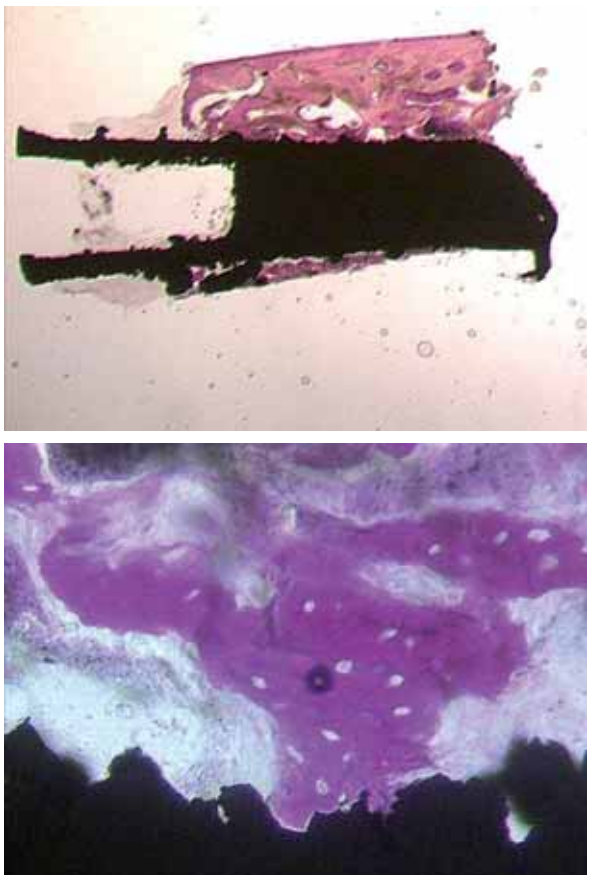

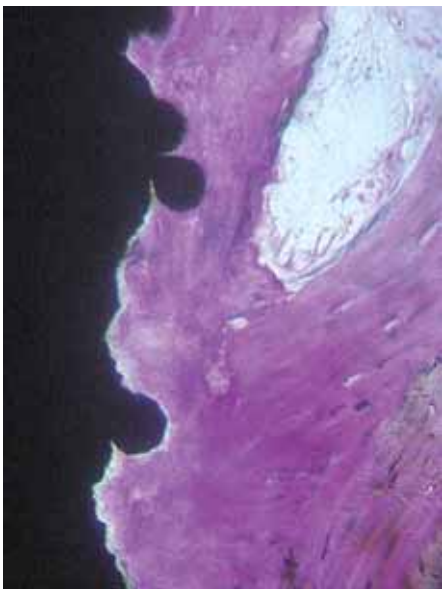

Fig. 2 DMLF surface.
A) Overview. The implant is surrounded by compact bone tissue, with small medullary areas.
B) At higher magnification compact bone with small medullary areas in contact with the implant surface. No gap at the interface can be detected, nor inflammatory response.
C) At higher magnification, new formed bone trabecula directly on the implant surface.

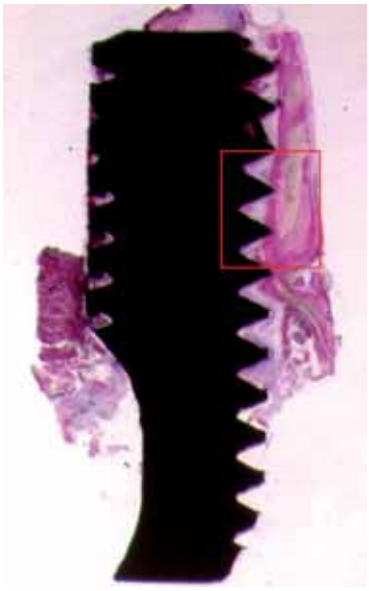

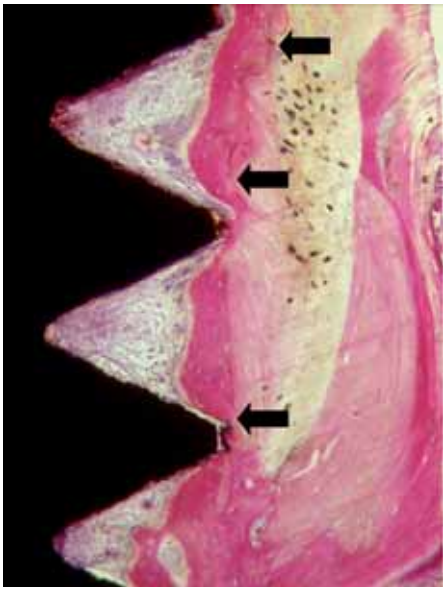

Fig. 3 cpTi surface.
a Overview. The lack of contact between the new formed bone trabeculae and the implant surface (basic fuchsin and toluidine blue 12 X).
b Magnification of the seleted area of the previous picture . The new formed bone shows no direct contact with the implant surface (basic fuchsin and toluidine blue 200X). Arrows highlight the parting between the new formed and the existing bone.

1). BIC and BDTA percentages were significantly lower ($p<0.05$) in cpTi implants. BIC% values for the cpTi surface ranged between 8.3% and 18.1%, with a mean 13.0%, while the values for the SAE and DLMF surfaces ranged between 18.4% and

	CPTI MEDIA ± DS RANGE	SAE MEDIA ± DS RANGE	DLMF MEDIA ± DS RANGE	P-VALUE	CI 95%
BIC%	13.06±5.74 8.34 – 18	21.81±3.72 18.8 – 25.26	23.29+2.91 18.4 – 27.6	0.0002	8.65 to 25.17
BDTA%	17.95±11.72 11.12 – 30	30.38±6.93 27.3 – 40	33.36±5.90 22.4 – 38.5	0.0052	8.58 to 39.66
BD%	14.88 ±7.69 10.3 – 26.7	15.37±6.22 2.31 – 22.8	15.37±5.66 2.1 – 20.22	0.999	8.96 to 20.70

Tab.1 Mean and standard deviation (DS) for percent values of bone-implant contact (BIC%), bone density in the threaded area (BDTA%) and bone density in a 300 micron wide area lateral to the implant (BD%), in machined surface (cpTi), sandblasted and acid surface implants (SAE) as well as laser produced (DLMF) placed in the posterior maxilla and logged at 2 months after placement. Kruskall-Wallis Test ($p<0.05$).

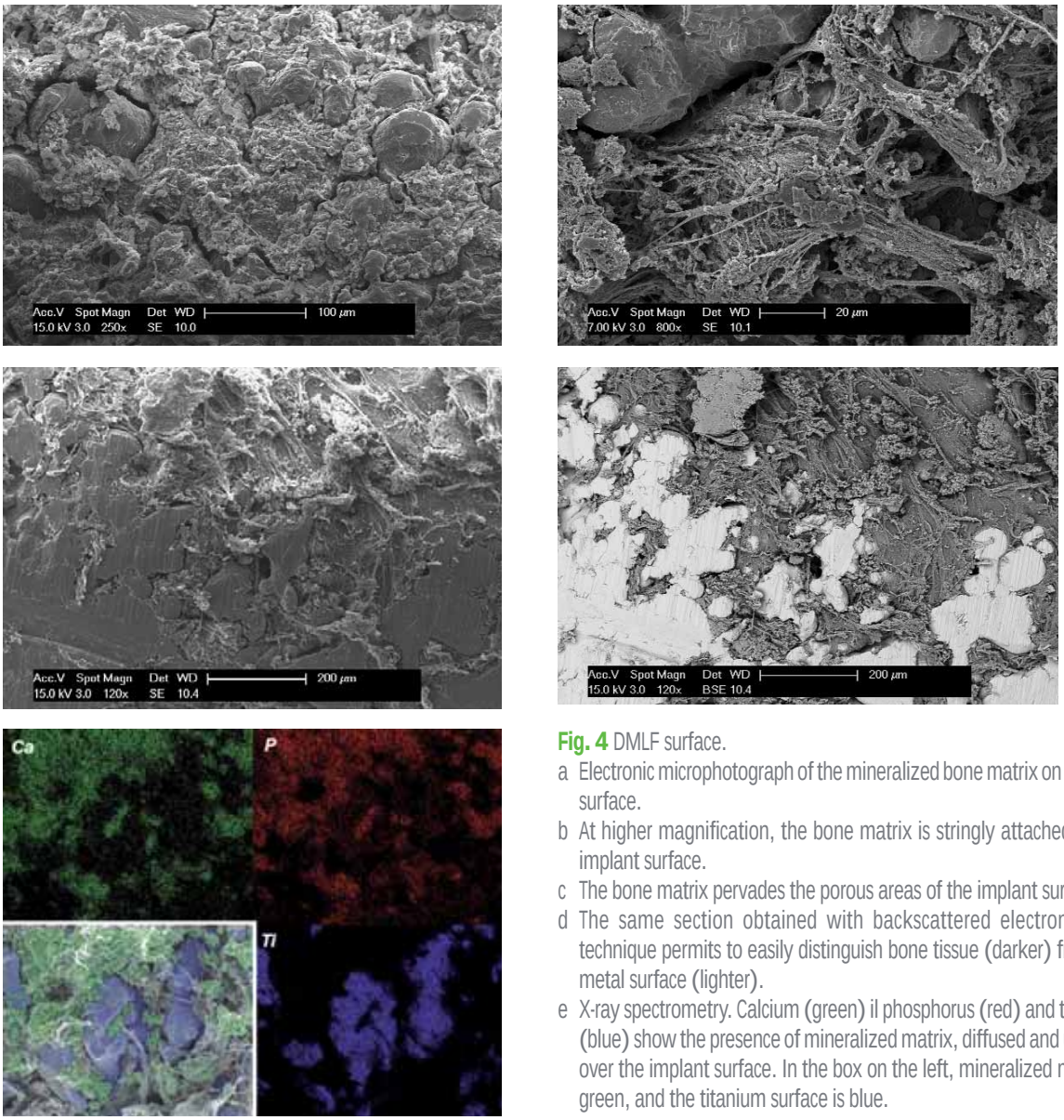

Fig. 4 DMLF surface.
a Electronic microphotograph of the mineralized bone matrix on implant surface.
b At higher magnification, the bone matrix is stringly attached to the implant surface.
c The bone matrix pervades the porous areas of the implant surface.
d The same section obtained with backscattered electrons. This technique permits to easily distinguish bone tissue (darker) from the metal surface (lighter).
e X-ray spectrometry. Calcium (green) il phosphorus (red) and titanium (blue) show the presence of mineralized matrix, diffused and uniform over the implant surface. In the box on the left, mineralized matrix is green, and the titanium surface is blue.

27.6%, with mean respectively of 21.8% and 23.2%. The mean BDTA for cpTi was 17.9% (range 11.1-30.0%); BDTA% for SAE and DLMF were comprised between 22.4% and 40.0%, with mean values respectively of 30.3% and 33.3%. Finally, the bone den-

sity in a 300 µm-wide zone lateral to the implant surface (BD%) was similar for all surface types, presenting mean values of about 15%

Scanning electron microscopy and X-Ray spectrometry

Scanning electron microscopy examination of DLMF specimens clearly showed the newly formed extracellular bone matrix infiltrating all the spaces among the peaks of the metal surface. The matrix was highly mineralized (Fig. 4a). The bone matrix was evidenced inside the concavities and irregular grooves of the specimen, in close connection with the surface (Fig. 4b), and it was not displaced even by the action, presumably traumatic, of the trephine bur (Fig. 4c-d). Osteoblasts presented a star shape with many slender cytoplasmic processes. The X-ray dispersive spectrometry made possible to underline the degree of mineralization of the newly formed bone matrix, mapping individual elements within the image. This aspect was evidenced in the four quadrants of the same picture, in which the distribution of calcium (green), phosphorus (red) and titanium (blue) was showed. The perfect co-localization of calcium and phosphorus, indicative of mineralized areas, was readily visible. The overlapping and combination of the images obtained with scanning electron microscopy to those of x ray dispersive spectrometry enforced the concept of a well organised, strongly mineralised bone matrix, in close connection with the surface of the implant (Fig. 4e).

DISCUSSION

In this histologic and histometric study on humans, the brand new surface of DLMF implants has shown an excellent degree of integration, with diffuse osteogenesis in close contact with the implant surface (25), two months after implant insertion. For this surface, BIC values were comprised between 18.4% e 27.6% (mean 23.2%), slightly superior to those obtained with SAE (range 18.8-25.2%, mean value 21.8%); all these results were statistically superior than those obtained with cpTi implants (range 8.3-18.1%, mean value 13.0%). Moreover, the optimal integration of DLMF surface was confirmed by data related to bone density in the threaded area (range 22.4- 38.5%, mean value 33.3%) slightly superior to those obtained with SAE (range 27.3-40.0%, mean value 30.3%) and considerably superior to those of cpTi surfaces (range 11.1-30.0%, mean value 17.1%). In particular, the newly formed bone was in close contact with the DLMF surface, presenting early stages of maturing and remodeling; on DLMF specimens, newly formed bone trabeculae were interposed between the pre-existing bone and the implant surface. These results were confirmed by the scanning electron microscopy examination and by x-ray spectrometry, where the amount of newly formed and highly mineralized bone matrix was evidenced, in close contact to the DLMF surface. What are the factors capable to influence early bone formation? It is noteworthy that the recruitment of osteogenic cells is fundamental for the deposition of new bone on the implant surface (25). Osteogenic cells are driven onto the implant surface through the established fibrin network around the implant. This is crucial to the early stages of osseointegration. Previous studies have indicated that there is a correlation between surface roughness and fibrin clot retention (26-27). As we have demonstrated in our previous in vitro study, the new porous DLMF surface is completely and immediately covered by a stable three dimensional fibrin network (9,11). On the other hand, the surface geometry and the open and interconnected pore microstructure of DLMF surface seems to represent the ideal environment for osteogenic cells (28-30). In a recent in vitro study with

human osteoblasts cultured on discs obtained by the laser fusion of titanium microparticles, Xue has investigated the behaviour of osteogenic cells in cavities and pores of different dimensions, ranging from 100-800 Ìm (28). In this study, cells did not penetrate into the cavities when the pores were <100 Ìm in diameter; on the other hand, for pores comprised between 100-200 Ìm in diameter, cells formed bridges upon cavities, spanning across intervening crevices by means of extended tightly stretched processes; for larger pores (>200 Ìm diameter), moreover, cells were capable to penetrate into cavities, and ingrowth of cells was observed in the interior of these larger pores. With pores with diameter >100 mm, in any case, Xue has evidenced the expression of specific markers of osteogenic phenotype expression, such as alkaline phosphatase, as well as matrix deposition (28). This was confirmed by our previous in vitro experience (9-11) with osteoblasts on porous surface of implants obtained by the fusion of titanium microparticles. In these studies, the same osteoblast behaviour has been evidenced, with strong evidence of bone matrix deposition. It is noteworthy that structural and geometric properties of surface can influence cell shape and size, with consequences on gene expression (31-34). Folkman (31) and Ingber (32) were the first researchers who underlined the importance of structural, mechanical and architectural features of cells. After fifteen years of research, mechanisms that relate cells shape to function have been partially elucidated (33). In fact, it is clear that cells interact with their substratum via integrins, specific linkage proteins (22-24, 33-35). Integrins are proteins related to the cellular membrane, and they are responsible for focal adhesion (23, 33-35). The formation of focal adhesion plaque is a prerequisite for the development of signalling transduction in cell adhesion. In fact, integrins are linked, through their cytoplasmic domain, to specific linkage proteins, such as alfa-actinin, talin, vinculina, paxilina and tensin. All these proteins are connected to the cytoskeleton (23-25, 28, 33-36). The cytoskeleton is the inner framework of cells. It is made up of three kinds of protein filaments: actin filaments (also called microfilaments), intermediate filaments (vimentin, desmin) and microtubules (tubulin). All these proteins are functionally interconnected and the cytoskeleton actively generates contractile forces, through the contraction of actin filaments (33-36). Since the cytoskeleton is functionally connected to the nucleus, it is not surprising that, through focal adhesion, mechanical forces applied from the substratum can be transformed into biochemical signals from cells (34-38). In fact, specific adhesion receptors linked to the deep cytoskeleton, such as integrins, cadherins and mechanoreceptors, if spatially and temporally “activated” from the geometry of the substratum, can provide preferred paths for mechanical signals to enter the cell, “activating” the mechanisms of trasduction. In this way, gene expression can be regulated by mechanical forced applied on the cell (33-38). Concavities seem to represent the ideal environment for osteogenic phenotype expression (34,39). In fact, the shape that cells are forced to adopt within the particular three dimensional microstructure of a cavity may create mechanical stresses that modulate gene expression (34,39). The cytoskeleton can integrate different signals because it is a mechanochemical scaffold that is both structure and catalyst. In fact, it is capable to translate mechanical forces into chemical signals, but it is also capable to modulate it because it is an active system, with its own peculiar contractile activity (33-38). In this sense, structure dictates function (31-34). Structural modifications and cytoskeletal rearrangements can influence the expression of the osteogenic phenotype (34). It happens also in nature, where bone

apposition occurs first in concavities (24,39). So, cells give peculiar responses to different geometrical features, and the laser microfusion technique permits to control fundamental parameters such as porosity, pore shape and size, pore distribution (28-30). It is noteworthy that an open and interconnected porosity is requested, as blood penetration inside the pore system is of fundamental importance. It is, in fact, a prerequisite for fluids, nutrients and oxygen supply, factors of paramount importance for osteoblast differentiation and new bone apposition (28-30,40); at the same time, this open pore architecture guarantees the discharge of the cell metabolic waste products (41). Nowadays, the microfusion of titanium permits to create surfaces which are capable to modulate specific biological and biomechanical responses.

CONCLUSIONI

In this comparative study on humans, the brand new surface (DLMF) of implants obtained from laser fusion of titanium microparticles (TixOs, Leader-Novaxa, Milan, Italy) has demonstrated to stimulate and to support new bone apposition, after an unloaded healing period of two months. The histologic and histometric result was superior to those obtained with conventional sandblasted, acid etched implants (SAE) and machined implants (cpTi). Scanning electron microscopy and x-ray spectrometry analysis confirmed these data, with evidence of early and diffuse mineralization of newly formed bone on DLMF surface. With direct laser fabrication (DLF) it is now possible to create implants with controlled surface geometry, incorporating a gradient of porosity, from the inner core to the outer surface. On the one hand, this kind of modulation can allow a better load adaptation and distribution; on the other hand, the presence of a ripetitive series of concavities of variable diameter (100-200 mm), extending and communicating within the porous spaces of which the outer implant portion is rich, seem to favour determined biological response, such as new bone apposition. The new era of microfuse titanium implants has began.

BIBLIOGRAFIA

1. Traini T, Mangano C, Sammons RL, Mangano F, Macchi A, Piattelli A. Direct laser metal sintering as a new approach to fabrication of an isoelastic functionally graded material for manufacture of porous titanium dental implants. Dental Materials 2008; 24: 1525-1533

2. Sykaras N, Iacopino AM, Marker VA, Triplett RG, Woody RD. Implant materials, design and surface topographies: their effect on osseointegration. A literature review. International Journal of Oral and Maxillofacial Implants 2000; 15: 675-690

3. Turner TM, Sumner DR, Urban RM, Rivero DP, Galante JO. A comparative study of porous coatings in a weight bearing total hip arthroplasty model. Journal of Bone and Joint Surgery America 1986; 68: 1396-1409

4. Kroger H, Venesmaa P, Jurvelin J, Miettinen H, Suomalainen O, Alhava E. Bone density at the proximal femur total hip arthroplasty. Clinical Orthopaedics and Related Resources 1998; 352: 66-74

5. Reilly DT, Burstein AH, Franklin VH. The elastic modulus of bone. Journal of Biomechanics 1974; 7:271-275

6. Rho JY, Roy ME, Tsui TY, Pharr GM. Elstic properties of microstructural components of human bone tissue as measured by nanoindentation. Journal of Biomedical Materials Research 1999; 45: 48-54

7. Lopez-Heredia MA, Sohier J, Gaillard C, Quillard S, Dorget M, Layrolle P. Rapid prototyped porous titanium coated with calcium phosphate as scaffold for bone tissue engineering. Biomaterials 2008; 29: 2608-2615

8. Hollander DA, von Walter M, Wirtz T, Sellei R, Schmidt-Rohlfing B, Paar O, Erli HJ. Structural, mechanical and in vitro characterization of individ-

ually structured Ti-6Al-4V implants produced by direct laser forming. Biomaterials 2006; 27: 955-963
9. Mangano C, Traini T, Piattelli A, Macchi A, Mangano A, Montini S, Mangano F. Impianti dentali in titanio sinterizzato tramite laser. Italian Oral Surgery 2006; 4: 7-12
10. Thieme M, Wieters KP, Bergner F, Scharnweber D, Worch H, Ndop J, Kim TJ, Grill W. Titanium powder sintering for preparation of a porous functionally graded material destined for orthopaedic implants. Journal of Materials in Science and Materials in Medicine 2001; 12: 225-231
11. Mangano C, Raspanti M, Traini T, Sammons R, Piattelli A. Stereo imaging and cytocompatibility of a model dental implant surface formed by direct laser fabrication. Journal of Biomedical Material Resources 2009, in press
12. Thomas KA, Cook S. An evaluation of variables influencing implant fixation by direct bone apposition. Journal of Biomedical Material Research 1985; 19: 875-901
13. Wong M, Eulenberger J, Schenck R, Hunziker E. Effect of surface topology on the osseointegration of implant materials in trabecular bone. Journal of Biomedical Material Research 1995; 29: 1567-1575
14. Carlsson L, Rostlund T, Albrektsson B, Albrektsson T. Removal torques for polished and rough titanium implants. International Journal of Oral and Maxillofacial Implants 1988; 3: 21-24
15. Wennenberg A, Albrektsson T, Albrektsson B. An animal study of commercially pure titanium screws with different surface topographies. Journal of Materials in Science and Materials in Medicine 1995; 6: 302-309
16. Boyan BD, Hummert TW, Kieswetter K, Schraub DM, Dean DD, Schwartz Z. Effect of titanium surface characteristics on chondrocytes and osteoblasts in vivo. Cell Materials 1995; 5: 323-335
17. Puleo DA, Nanci A. Understanding and controlling the bone-implant interface. Biomaterials 1999; 20: 2311-2321
18. Wieland M, Textor M. Measurement and evaluation of the chemical composition and topography of titanium implant surfaces in design. In: Davies JE, editor, Bone Engineering, Toronto 2000; pp. 163-182
19. Rupp F, Scheideler L, Rehbein D, Axmann D, Geis-Gerstorfer J. Roughness induced dynamic changes of wettability of acid etched titanium implant modification. Biomaterials 2004; 25: 1429-1438
20. Mangano C, Ripamonti U, Piattelli A, Mangano F, Montini S. La bioingegneria applicata all'implantologia osteointegrata: realtà clinica o ricerca pura? Implantologia Orale 2006; 1: 47-56
21. De Bruijin JD, van Blitterswijk CA, Davies JE. Initial bone matrix formation at the hydroxyapatite interface in vivo. Journal of Biomedical Material Research 1995; 29: 89-99
22. Nanci A, Zalzal S, Fortin M, Mangano C, Goldberg HA. Incorporation of circulating bone matrix proteins by implanted hydroxyapatite and at the bone surfaces: implications for cement line formation and structuring of biomaterials. In: Davies JE, editor, Bone Engineering, Toronto 2000; pp. 305-311
23. Gronowicz G, Mc Carthy MB. Response of human osteoblasts to implant materials: Integrin-mediated adhesion. Journal of Orthopaedic Research 1996: 4 878-887
24. Mangano C, Ripamonti U, Mangano F, Montini S, Martinetti R. Ingegneria Tessutale, induzione ossea e biomateriali biomimetici. Implantologia Orale 2004; 5: 9-35
25. Davies JE. Mechanisms of endosseous integration. International Journal of Prosthodontics 1998; 11: 391-401
26. Di Iorio D, Traini T, Degidi M, Caputi S, Neugebauer J, Piattelli A. Quantitative evaluation of the fibrin clot extension on different implant surfaces: an in vitro study. Journal of Biomedical Material Resources B Applied Biomaterials 2005; 74: 636-642
27. Park JY, Gemmel CH, Davies JE. Platelet interactions with titanium: modulation of platelet activity by surface topography. Biomaterials 2001; 22: 2671-2682
28. Xue W, Krishna V, Bandyopadhyay A, Bose S. Acta Biomaterialia 2007; 3: 1007-1018
29. Ryan G, Pandit A, Apatsidis DP. Fabrication methods of porous metals for use in orthopaedic applications. Biomaterials 2006; 27: 2651-2670
30. Leong KF, Cheah CM, Chua CK. Solid freeform fabrication of three dimensional scaffolds for engineering replacement tissues and organs. Biomaterials 2003; 24: 2363-2378
31. Folkman J, Moscona A. Role of cell shape in

growth control. Nature 1978; 273: 345-349
32. Ingber D. The architecture of life. Scientific American 1998; 48: 48-59
33. Ingber D. From molecular cell engineering to biologically inspired engineering. Cellular and Molecular Bioengineering 2008; 1: 51-57
34. Ripamonti U. Soluble, insoluble and geometric signals sculpt the architecture of mineralized tissues. Journal of Cell Molecular Medicine 2004; 8: 169-180
35. Anselme K. Osteoblast adhesion on biomaterials. Biomaterials 2000; 21: 667-681
36. Cretel E, Pierres A, Benoliel AM, Bongrand P. How cells feel their environment: a focus on early dynamic events. Cellular and Molecular Bioengineering 2008; 1: 5-14
37. Janmey PA. The cytoskeleton and cell signalling: component localization and mechanical coupling. Physiology Reviews 1998; 78: 763-781
38. Wang N, Butler JP, Ingber D. Mechanotrasduction accross the cell surface and through the cytoskeleton. Science 1993; 260: 1124-1127
39. Mangano C, Perrotti V, Iezzi G, Scarano A, Mangano F, Piattelli A. Bone response to new modified titanium surface implants in non-human primates (Papio Ursinus) and humans: histological evaluation. Journal of Oral Implantology 2008; 1: 17-24
40. Le Geros RZ, Le Geros JP. Calcium phosphate biomaterials: preparation, properties and biodegradation. In Wise DL, Trantolo DJ, Altobelli DE, Schwartz ER eds., Encyclopedia handbook of biomaterials and bioengineering part A: materials, vol.2. New York, Marcel Dekker 1995, p. 1429-1463
41. Vacanti JP, Morse MA, Saltzmann WM, Domb AJ, Peter-Atayde A, Langer R. Selective cell transplantation using bioresorbable artificial polymers as matrices. Journal of Paediatric Surgery 1988; 23: 3-9.